AD-A088 082 NAVAL RESEARCH LAB WASHINGTON DC F/G 8/3
ON THE INFERENCE OF OCEANIC CURRENTS OR EDDIES BY SPACEBORNE AL--ETC(U)
JUL 80 D T CHEN, V E NOBLE
UNCLASSIFIED NRL-MR-4273 NL

1 OF 1
AD A088082

END
DATE FILMED
9-80
DTIC

AD A088082

On The Inference of Oceanic Currents by Spaceborne Altimetry Through the Dynamic Method for the Determination of Three-Dimensional Density (Temperature) Field

Space Systems Division

18 July 1980

W05270500

NAVAL RESEARCH LABORATORY
Washington, D.C.

SECURITY CLASSIFICATION OF THIS PAGE *(When Data Entered)*

REPORT DOCUMENTATION PAGE		READ INSTRUCTIONS BEFORE COMPLETING FORM
1. REPORT NUMBER NRL Memorandum Report 4273	2. GOVT ACCESSION NO. AD-A088	3. RECIPIENT'S CATALOG NUMBER 082
4. TITLE *(and Subtitle)* ON THE INFERENCE OF OCEANIC CURRENTS OR EDDIES BY SPACEBORNE ALTIMETRY THROUGH THE DYNAMIC METHOD FOR THE DETERMINATION OF THREE DIMENSIONAL DENSITY (TEMPERATURE) FIELD		5. TYPE OF REPORT & PERIOD COVERED Progress Report 6. PERFORMING ORG. REPORT NUMBER
7. AUTHOR(s) Davidson T. Chen and Vincent E. Noble		8. CONTRACT OR GRANT NUMBER(s)
9. PERFORMING ORGANIZATION NAME AND ADDRESS Naval Research Laboratory Washington, D.C. 20375		10. PROGRAM ELEMENT, PROJECT, TASK AREA & WORK UNIT NUMBERS 79-0932-0-0; AIRTASK A370-370G/058C/0W0527OS00; 63207N
11. CONTROLLING OFFICE NAME AND ADDRESS		12. REPORT DATE July 18, 1980 13. NUMBER OF PAGES 32
14. MONITORING AGENCY NAME & ADDRESS *(if different from Controlling Office)*		15. SECURITY CLASS. *(of this report)* UNCLASSIFIED 15a. DECLASSIFICATION/DOWNGRADING SCHEDULE

16. DISTRIBUTION STATEMENT *(of this Report)*

Approved for public release; distribution unlimited.

17. DISTRIBUTION STATEMENT *(of the abstract entered in Block 20, if different from Report)*

DTIC ELECTE S AUG 19 1980 D B

18. SUPPLEMENTARY NOTES

19. KEY WORDS *(Continue on reverse side if necessary and identify by block number)*

Geostrophic currents and eddies
Dynamic method
Spaceborne altimeter
Bounded and unique solution
Three dimensional density (temperature) field

20. ABSTRACT *(Continue on reverse side if necessary and identify by block number)*

The physical theoretical background, the mathematical governing equations, the absolute error, and the relative error of the dynamic method used in inferring the geostrophic current and eddy systems from the spaceborne altimeter-sensed measurements of dynamic heights or slopes have been laboriously developed. And, also, the conditions for the determination of the three dimensional density (temperature) field uniquely are mentioned and explained. The spaceborne altimeter is shown to be the instrument for the provision of one condition, i.e., the ocean surface current condition. The three-dimensional density (temperature) field and its boundary conditions at the air-sea interface play dominent roles in the weather prediction and the undersea technology. The interchangeable use of the terms of density and temperature fields is valid only when the salinity can be assumed as constant. (Abstract continues)

DD FORM 1 JAN 73 1473 EDITION OF 1 NOV 65 IS OBSOLETE
S/N 0102-LF-014-6601

SECURITY CLASSIFICATION OF THIS PAGE *(When Data Entered)*

20. (Abstract continued)

Memo #205

This report complements the previous report by Chen, et al., [1980] in which the requirements on the measurement error of the dynamic heights or slopes by the spaceborne altimeter are defined. It is hoped that these two reports will help to clearly establish the mission priorities and requirements for future satellite systems.

CONTENTS

ON THE INFERENCE OF OCEANIC CURRENTS OR EDDIES BY SPACEBORNE ALTIMETRY THROUGH THE DYNAMIC METHOD FOR THE DETERMINATION OF THREE DIMENSIONAL DENSITY (TEMPERATURE) FIELD

I. INTRODUCTION

The majority of oceanic features such as currents and eddies not only exhibit measurable temperature gradients at both the surface and subsurface level [Stommel, 1966; Stommel and Yoshido, 1972; Bruce, 1979; Halliwell and Mooers, 1979; Richardson, et al., 1979; Vukovich and Crissman, 1979], but also possess measurable dynamic heights and slopes [Stommel, 1966; Stommel and Yoshido, 1972; Vukovich and Crissman, 1979]. These dynamic heights and slopes are the results of different density and current profiles in the horizontal and vertical directions through the currents and the eddies. These dynamic heights and slopes are the deviations from the local geoid heights and slopes which, theoretically, represent a motionless ocean. The dynamic slopes as well as the variations of dynamic heights can induce horizontal pressure gradients. Under the steady state situation, by neglecting the effects due to friction and removing the effects due to wind set-up and atmosphere pressure, one may relate the geostrophic current velocity orthogonally to the horizontal pressure gradient by the dynamic method. In the case of eddies the horizontal pressure gradient is further balanced by the centrifugal force. Therefore, under the geostrophic approximation, one is able to evaluate the current velocity field if the dynamic heights and slopes over the current are known.

A satellite microwave altimeter obtains its range measurement by determining the round trip travel time of a narrow pulse of electromagnetic energy from the radiating antenna to the scattering surface and back [McGoogan, 1975; Cutting, et al., 1977]. In practice, the round trip travel time is determined by the separation, on the time axis, between an arbitrarily chosen reference point and an identifiable point on the return, usually the midpoint of the ramp section of the return pulse. The determined range should be corrected for atmospheric and ionospheric propagation errors. The instantaneous ocean surface topography is determined by subtracting the altimeter range measurement from the (precisely determined) satellite position. The local dynamic height is derived from the instantaneous ocean surface topography after corrections attributed to the marine geoid, tides, barometric pressure, wind set-up and storm surges [Chen, et.al., 1980]. Therefore, spaceborne altimeter measurements can be used to infer current and eddy systems and delineate their boundaries [Huang, et al, 1978; Leitao, et al., 1979].

Theoretically, a complete set of conditions required for a mathematically and physically unique and bounded current velocity field are well defined. These conditions, derived from the Euler's equation of motion and the equation for continuity of fluids, are the known bottom topography, the known vertical and horizontal density profiles, and the known surface kinematic and dynamic conditions. In other words, if the current velocity field is known the unknown three-dimensional density field can be uniquely determined. Although the spaceborne altimeter measurements can only be used to infer, within the instrument's precision, those geostrophic currents whose physical locations are outside the latitude band of 20° south to 20° north this all-weather spaceborne altimeter can provide global information on the majority of current systems and eddies. Furthermore, with the additional information on the sea surface temperature provided by the synoptic two-dimensional spaceborne infrared sensor, the chance of obtaining the complete conditions or field equations is greatly enhanced globally and synoptically. Obviously useful information can be derived readily. For example, one

can assume an initial three-dimensional density field over an area and be confident that these assumed density profiles (which constitute the density field) will converge uniquely to the desired actual density profiles at the end of his mathematical manipulations. Information on the synoptically detected currents, eddies, and their physical locations by the spaceborne altimeter will benefit acoustic propagation predictions.

It is indeed important that one should not only know how this dynamic method is derived theoretically, but also know the limitations and the errors of this method in deriving the current velocity field from the known dynamic heights or slopes. These two areas of concern will be described briefly in the following sections.

The determination of a three dimensional density (temperature) field by using the altimeter measurements will also be discussed. The interchangeable use of density field and temperature field is valid only when the salinity is assumed to be constant.

II. DYNAMIC METHOD

Subtracting the corrected spaceborne altimeter range measurements, corrections for the atmospheric and the ionspheric propagation errors from the independently measured satellite orbit, the remainder is the altimeter-sensed sea level. Referring to the geoidal reference ellipsoid [Chen, et al., 1980], the altimeter-sensed sea level ζ_S can be expressed as:

$$\zeta_S(\vec{r}) = \zeta_R\ (p_a(\vec{r}),\rho(\vec{r}),\vec{\omega}(\vec{r}),\vec{q}(\vec{r}),\vec{A}(\vec{r})) + G(\vec{r}) \qquad (2.1)$$

where G is the Geoid, $\vec{r}$ is the position vector, ζ_R is the sea level as the perturbation to the Geoid, p_a is the atmospheric pressure, ρ is the density of the water column directly under the sea surface, $\vec{\omega}$ is the surface wind vector, $\vec{q}$ is the current velocity and $\vec{A}$ is the astronomical forces (which generate tides). The expression for ζ_R in Equation (2.1) is certainly a complicated one. Nevertheless, the effects on ζ_R due to

p_a, $\vec{\omega}$, and $\vec{A}$ such as barometric, wind set-up, storm surge, and tidal sea level variations can be removed with independent measurements. Therefore, Equation (2.1) does reduce to

$$\zeta_R(\vec{r}) \rightarrow \zeta(\vec{r}) = \zeta(\rho(\vec{r}), \vec{q}(\vec{r})) \tag{2.2}$$

where ζ is the mean sea level in the traditional sense. Physical oceanographers would like to call ζ the mean sea level with respect to an arbitrary datum. However, one would be legitimately concerned about the effectiveness of reducing Equation (2.1) to Equation (2.2) for ζ, especially the higher order terms. Fortunately, most of the parameters for ζ_R act on different time scales, and proper averaging can lead to meaningful interpretations for ζ in Equation (2.2). For example, the astronomical forces have well defined periods of days or months. Therefore, the influences of transient events on ζ due to p_a, $\vec{\omega}$, and $\vec{A}$ can be removed and the contributions to ζ by the quasi-permanent features of ρ and $\vec{q}$ as shown in Equation (2.2) along the major ocean current system remain in the data. This procedure has been demonstrated successfully by the GEOS-3 investigation on the Gulf Stream [Huang, et al., 1978].

In most cases, the ocean density structure, which requires in situ measurements for unique determination can be related to the current by geostrophic assumptions. But if barotropic motion is further assumed, the current can be related directly to mean sea level slope or the mean dynamic slope.

Assuming a linear constitutive law for the surface strain rate tensor the basic hydrodynamic equations describing oceanic circulation in a general time dependent case are [Hill, 1962], the Euler's equation of motion,

$$\frac{\partial \vec{q}(\vec{r})}{\partial t} + (\vec{q}(\vec{r})\cdot\vec{\nabla})\vec{q}(\vec{r}) + 2\vec{\Omega}\times\vec{q}(\vec{r}) + \vec{\omega}\times(\vec{\omega}\times\vec{r}) = -\frac{1}{\rho(\vec{r})}\vec{\nabla}p(\vec{r}) + \vec{b}(\vec{r}) + \nu\nabla^2\vec{q}(\vec{r}) \tag{2.3a}$$

and, the equation of continuity,

$$\frac{\partial \rho(\vec{r})}{\partial t} + \vec{\nabla}\cdot(\rho(\vec{r})\vec{q}(\vec{r})) = 0 \qquad (2.3b)$$

with the associated kinematic and dynamic boundary conditions. In Equations (2.3a) and (2.3b), $\vec{q}$ is the velocity, $\vec{\Omega}$ is the angular velocity of the earth, $\vec{\omega}$ is the angular velocity of the eddy, $\vec{r}$ is the position vector of the fluid, ρ is the density of sea water, p is the pressure, $\vec{b}$ is the body force, and ν is the kinematic viscosity of the sea water. The position vector $\vec{r}$ is a function of time t. The third term on the left hand side, $2\vec{\Omega} \times \vec{q}$, of Equation (2.3a) is the Coriolis force induced by the fluid motion $\vec{q}$ and the fourth term, $\vec{\omega}\times(\vec{\omega}\times\vec{r})$, is the centrifugal force induced by the eddy motion. In the absence of eddy motion the centrifugal force term always vanishes. Notice that Equations (2.3a) and (2.3b) are differential equations for the geometric components for the steady state situation, Equations (2.3a) and (2.3b) become

$$(\vec{q}(\vec{r})\cdot\vec{\nabla})\vec{q}(\vec{r}) + 2\vec{\Omega}\times\vec{q}(\vec{r}) + (\vec{\omega}\cdot\vec{r})\,\vec{\omega} - (\vec{\omega}\cdot\vec{\omega})\vec{r}$$

$$= -\frac{1}{\rho(\vec{r})}\vec{\nabla}p(\vec{r}) + \vec{b}(\vec{r}) + \nu\nabla^2\vec{q}(\vec{r}) \quad , \qquad (2.4a)$$

and

$$\vec{q}\cdot\vec{\nabla}\rho(\vec{r}) + \rho(\vec{r})\vec{\nabla}\cdot\vec{q}(\vec{r}) = 0 \quad . \qquad (2.4b)$$

With the Boussinesq, the hydrostatic, the Rectangular Cartesian Coordinates', and the scale approximations and, also, the eddy term assumption, Equations (2.4a) and (2.4b) are further reduced to the component form as

$$2\sin\lambda|\vec{\Omega}|q_2(\vec{x}) - \omega_i x_i \omega_1 + |\vec{\omega}|^2 x_1 = \frac{1}{\rho(\vec{x})}\frac{\partial p(\vec{x})}{\partial x_1} \quad , \; i = 1, 2, 3, \qquad (2.5a)$$

$$2\sin\lambda|\vec{\Omega}|q_1(\vec{x}) + \omega_i x_i \omega_2 - |\vec{\omega}|^2 x_2 = -\frac{1}{\rho(\vec{x})}\frac{\partial p(\vec{x})}{\partial x_2} \quad , \; i = 1, 2, 3, \qquad (2.5b)$$

$$0 = \frac{1}{\rho(\vec{x})}\frac{\partial p(\vec{x})}{\partial x_3} - g \quad , \qquad (2.5c)$$

and

$$\frac{\partial q_1(\vec{x})}{\partial x_1} + \frac{\partial q_2(\vec{x})}{\partial x_2} = 0 \quad . \tag{2.5d}$$

respectively, where $\vec{x} = (x_1, x_2, x_3)$ is the position vector, λ is the latitude (positive in northern hemisphere) and g is the gravitational acceleration. The Cartesian Coordinates x_1, x_2, and x_3 are in the local east, north, and vertical downward directions. However, since usually

$$\vec{\omega} = (0, 0, \omega_3) \tag{2.6}$$

Equations (2.5a), (2.5b), (2.5c), and (2.5d) can be simplified as

$$2\sin\lambda|\vec{\Omega}|q_2(\vec{x}) + \omega_3^2 x_1 = \frac{1}{\rho(\vec{x})}\frac{\partial p(\vec{x})}{\partial x_1} \quad , \tag{2.6a}$$

$$2\sin\lambda|\vec{\Omega}|q_1(\vec{x}) - \omega_3^2 x_2 = -\frac{1}{\rho(\vec{x})}\frac{\partial p(\vec{x})}{\partial x_2} \quad , \tag{2.6b}$$

$$\frac{\partial p(\vec{x})}{\partial x_3} = \rho(\vec{x})g \quad , \tag{2.6c}$$

and

$$\frac{\partial q_1(\vec{x})}{\partial x_1} + \frac{\partial q_2(\vec{x})}{\partial x_2} = 0 \quad . \tag{2.6d}$$

Equations (2.6a) and (2.6b) are the typical differential equations for dynamic systems, which can readily be solved by the method of complex variables. Equation (2.6c) is nothing but the hydrostatic equation and equation (2.6d) is the continuity equation in the horizontal plane.

In the actual case of eddy motion,

$$\omega_3 = \pm\left[\frac{q_1^2(\vec{x}) + q_2^2(\vec{x})}{x_1^2 + x_2^2}\right]^{1/2} \tag{2.7}$$

where ω_3 can either be positive or negative according to the right hand rule. For the sake of discussion, let ω_3 be positive. Equations (2.6a)

and (2.6b) then have the forms of

$$2\sin\lambda|\vec{\Omega}|q_2(\vec{x}) + \left[\frac{q_1^2(\vec{x}) + q_2^2(\vec{x})}{x_1^2 + x_2^2}\right] x_1 = \frac{1}{\rho(\vec{x})}\frac{\partial p(\vec{x})}{\partial x_1} \quad , \qquad (2.8a)$$

and

$$2\sin\lambda|\vec{\Omega}|q_1(\vec{x}) - \left[\frac{q_1^2(\vec{x}) + q_2^2(\vec{x})}{x_1^2 + x_2^2}\right] x_2 = -\frac{1}{\rho(\vec{x})}\frac{\partial p(\vec{x})}{\partial x_2} \quad . \qquad (2.8b)$$

With a coordinate transformation from the Rectangular Cartesian Coordinates to the local cylindrical coordinates Equations (2.8a), (2.8b), (2.6c) and (2.6d) become, under the assumption of $\vec{q} = \vec{q}(x_1)$,

$$2\sin\lambda|\vec{\Omega}||\vec{q}(x_1)| + \frac{|\vec{q}(x_1)|^2}{x_1} = \frac{1}{\rho}\frac{\partial p}{\partial x_1} \quad , \qquad (2.9a)$$

$$\frac{1}{\rho}\frac{\partial p}{\partial x_2} = 0 \quad , \qquad (2.9b)$$

$$\frac{1}{\rho}\frac{\partial p}{\partial x_3} = g \quad , \qquad (2.9c)$$

and

$$\frac{\partial|\vec{q}(x_1)|}{\partial x_1} = 0 \qquad (2.9d)$$

where x_1 is in the radial direction from the center of the eddy, x_2 is in the counterclockwise angular direction and x_3 is in the vertical downward direction. It is quite obvious that the current is in an axisymmetric pattern and

$$|\vec{q}(x_1)| = x_1\frac{\partial x_2}{\partial t} = x_1\omega_3 \qquad (2.10)$$

with respect to Equation (2.7).

Nevertheless the second terms at the left hand sides of equations (2.8a) and (2.8b) are high order terms, for current systems other than eddies, these terms can be dropped as

$$2\sin\lambda|\vec{\Omega}|q_2(\vec{x}) = \frac{1}{\rho(\vec{x})}\frac{\partial\rho(\vec{x})}{\partial x_1} \quad , \tag{2.11a}$$

and

$$2\sin\lambda|\vec{\Omega}|q_1(\vec{x}) = -\frac{1}{\rho(\vec{x})}\frac{\partial p(\vec{x})}{\partial x_2} \quad . \tag{2.11b}$$

Equations (2.11a), (2.11b), (2.6c), and (2.6d) are the governing equations for the geostrophic current system. Although these equations do not include the centrifugal terms which render them unfit for eddy systems, these equations will be used, henceforth, without the loss of generality and rigor. The method which uses Equations (2.11a), (2.11b), (2.6c), and (2.6d) for inferring current from the dynamic heights or slopes is called the dynamic method.

Several important comments concerning the use of this dynamic method are required to be made:

1. From Equations (2.11a) and (2.11b) it is quite important to bear in mind that the effects on the current system due to frictional forces such as those induced by wind have not been considered. The wind effect is assumed to be in the form of wind set-up which has been assumed to be removed by independent means. However, wind action on the sea surface lead to the horizontal inhomogeneity of water density and to the appearance of a gradient current [Fomin, 1964]. The total steady gradient current is computed by the dynamic method also.
2. The gradient component of a steady current is computed by the dynamic method from the distribution of sea water density. This component of current velocity is induced by the horizontal pressure gradient. From Equation (2.6c),

$$p(\vec{x}) - \bar{p}_a(\vec{x}) = g\int_{\zeta}^{x_3}\rho(\vec{x})dx_3 \tag{2.12}$$

where $\tilde{p}_a$ is the reference atmospheric pressure at the mean sea surface ζ. Using Leibniz rule

$$\frac{\partial p(\vec{x})}{\partial x_1} = g \int_{\zeta}^{x_3} \frac{\partial \rho(\vec{x})}{\partial x_1} dx_3 - g\rho(\zeta) \frac{\partial \zeta}{\partial x_1} \tag{2.13}$$

where $\rho(\zeta)$ is water density at the sea surface. Equation (2.13) shows that the horizontal pressure gradient consists of two components. One is due to the horizontal inhomogeneity of the water density field and depends largely on the vertical coordinates, while the other results from the slope of the free surface of the sea and does not change along the vertical. It is quite easy to see that the spaceborne altimeter is capable of measuring the second term of the right hand side of Equation (2.13). The horizontal inhomogeneity of the water density field is required to be provided by independent means such as those provided by the combination of infrared and acoustic sensors.

3. In the dynamic method, it is assumed that at a certain depth the horizontal pressure gradient and current velocity are zero. This depth can also be defined at where the two components of the horizontal pressure gradient, shown by Equation (2.13), are mutually compensated. To underline the importance of having such a depth, but without knowing where it is, let us introduce the Helland-Hansen and Ekman Theorem [Fomin, 1964] of the Parallelism of Solenoids in the sea. The dynamic method is based on this theorem. Helland-Hansen and Ekman Theorem of the Parallelism of Solenoids says: <u>If the motion of the sea water is stationary, the heat content, salinity, and amount of movement in a volume of water remain constant during motion and the water moves along an isobaric (or equipotential) surface, then the isotherms, isohalines, isotachs, and dynamic isobaths lying on the isobaric (or equipotential) surface are streamlines at this surface. If these isolines are orthogonally projected from one isobaric (or equipotential) surface on another, they will coincide with the isolines on the latter surface</u>. Haiami, et al., [1955] have shown that the computation of currents by the dynamic method does not require preliminary determination of the depth of the no motion layer or knowledge of current

velocity at some surface if this Theorem is satisfied.

III ACCURACY OF THE DYNAMIC METHOD

The absolute error in the computation of current velocity from Equations (2.11a), (2.11b), (2.6c) and (2.6d) can be estimated by the exact differentials to be, numerically,

$$d|\vec{q}(\vec{x}_{i+1})| = \frac{g}{2\sin\lambda|\vec{\Omega}||\vec{x}_{i+1} - \vec{x}_i|}\, d[\zeta(\vec{x}_i)-\zeta(\vec{x}_{i+1})]$$

$$+ \frac{g[\zeta(\vec{x}_i) - \zeta(\vec{x}_{i+1})]}{2\sin\lambda|\vec{\Omega}||\vec{x}_{i+1} - \vec{x}_i|^2}\, d|\vec{x}_{i+1}-\vec{x}_i| \qquad (3.1)$$

where the position vectors $\vec{x}_{i+1}$ and $\vec{x}_i$ are in the finite difference sense and the symbol "d" denotes measurement errors. These measurement error terms at the right hand side of Equation (3.1) are readily available from the spaceborne altimeter and tracking instrument specifications such as those provided for SEASAT-A Oceanographic Satellite [Cutting, et al., 1977; Colquitt, et al., 1979; Tapley, et al., 1979]. The error induced in the current calculation increases with increasing distance between the reference, i.e. the "zero" current depth, and the given mean sea surface, and with decreasing geographical latitude of the area λ and distance between measurements $|\vec{x}_{i+1}-\vec{x}_i|$. In their study, Chen, et al., [1980] assume uniformly distributed errors in the position determination, the second term on the right hand side of Equation (3.1) is, thus, identically zero.

The absolute error in the computation of current velocity as such can not characterize the degree of accuracy of the result obtained. The same absolute error will confirm the great reliability of the pattern of horizontal circulation when current velocities are high, whereas with low velocities it indicates that it is impossible to obtain an idea of currents by the dynamic method. Therefore, it is more realistic to use the relative error in the computation of current velocity when estimating the reliability of the computed current velocities. The relative

error is defined as $d|\vec{q}(\vec{x}_{i+1})| \Big/ |\vec{q}(\vec{x}_{i+1})|$ where the numerator is given by Equation (3.1) and the denominator comes from Equations (2.11a), (2.11b), (2.6c), and (2.6d).

IV. DETERMINATION OF THREE DIMENSIONAL DENSITY (TEMPERATURE) FIELD

Recent observations [MODE GROUP, 1978] have demonstrated, significantly, that most of the kinetic energy of the ocean circulation is associated with variability on a relatively small scale, the mesoscale, of the order of 100 km. In other words, the current field which transports heat, nutrients, and salt contents in the ocean not only varies quite a bit in amplitude, but also varies in a spatial dimension which is comparable to 100 km in length. These types of variability and spatial dimension exhibited in the current field have important implications in weather prediction, and undersea technology such as sound propagation [Shear, 1971; James, 1972; Vastano and Owens, 1973; Lavenson and Doblar, 1976]. By assuming constant salinity it becomes necessary to quantify the ocean by four independent physical parameters which are the current velocity $\vec{q}(\vec{r})$, the pressure $p(\vec{r})$, the density $\rho(\vec{r})$, and the temperature $T(\vec{r})$. The physical parameters $\vec{q}$ and T together with the energy exchange between the ocean and the atmosphere are the critical elements involved in weather prediction while the physical parameters p, ρ and T are the important quantities for undersea acoustics, for example. In order to quantify mesoscale phenomena, of 100 km in dimension, with an acceptable error for the various applications, a horizontal resolution of 5 km and a vertical resolution varying from 1 m to 1 km are required. The definite vertical resolution [Clancy and Martin, 1979] depends, however, on the magnitude of vertical density gradient. In the mixing layer, for example, where the vertical density gradient is not very large, the vertical resolution can be 5 m at the top and is reduced down to 1 m where the mixing layer meets the thermocline.

Nevertheless, on the mathematical and the physical grounds, in order to guarantee the uniqueness and the convergence of these four physical parameters, a set of conditions are required to be satisfied

[Hill, 1962; Neumann and Pierson, 1966]:

1. The three dimensional descriptions of the field is required to be specified: Based upon the principles of conservation of momentum and conservation of mass, Equations (2.3a) and (2.3b) are derived for the four physical parameters $\vec{q}$, p, ρ, and T. However, since $\vec{q}$ is a vector, six independent equations are required to specify the field. Besides the four equations provided by Equations (2.3a) and (2.3b) two more equations should be added. One equation is called the equation of state,

$$\rho(\vec{r}) = \rho(S(\vec{r}),\ T(\vec{r})) \tag{4.1}$$

where the salinity $S(\vec{r})$ has been assumed to be constant. And the other equation describing the change in temperature is

$$\frac{\partial T(\vec{r})}{\partial t} + (\vec{q}(\vec{r}) \cdot \vec{\nabla})T$$

$$= K\nabla^2 T + \nu \left\{ \vec{\nabla} \cdot [(\vec{q}(\vec{r}) \cdot \vec{\nabla})\vec{q}(\vec{r})] - \frac{2}{3}(\vec{\nabla} \cdot \vec{q})^2 \right\}$$

$$+ Q(\vec{r}) \tag{4.2}$$

Where K is the coefficient for the molecular diffusion of heat, ν is the coefficient of kinematic viscosity and Q is the source strength for the energy that causes the fluid to change its temperature. Equations (2.3a), (2.3b), (4.1), and (4.2) are complicated equations to be solved indeed. With the multiple layers approach, quite a few numerical modelling techniques are proved to be partially successful in solving these equations. The problem area remaining at present, however, is the lack of adequate description of energy transfer at the air-sea interface. The multiple-layered model, described and analyzed by Clancy and Martin [1979], has the potential to overcome this problem by using satellite-observed information on the ocean surface temperature. By the way, if the salinity cannot be assumed as a constant, one more equation is required to be added to fully describe the field. A mean Temperature-

Salinity curve [Emery, et al., 1979] for the area surveyed can also be used to delineate density profiles from temperature profiles as the opportunity arises.

2. The energy exchange at the air-sea interface must be specified: The energy exchange at the air-sea interface involves two types. The first type is the exchange of kinetic and potential energy. The other type is the exchange of heat energy. With the removal of the effects due to wind set-up, storm surge and atmospheric pressure by the method mentioned in Section II for this interface, the first type of energy exchange is reduced to that involved in the wind-current and wind-wave interactions. The physical mechanisms involved in the wind-current and wind-wave interactions are quite complicated. By assuming a flat ocean surface, statistical descriptions which require the assumptions for the eddy terms in Equation (2.3a) have been used successfully [Neumann and Pierson, 1966] in describing the energy exchange between the wind and the current.

The second type of energy exchange is also complicated [Jacobs, 1951]. Not only the incident, reflected, and refracted solar energy at this interface are required to be known, but also the temperature profiles at both sides of the interface as well as the atmospheric moisture content are required to be known. Several model equations are currently under investigations for this type of energy exchange. Measurements required for these parameters are very difficult to make and obtain. Because of these difficulties the progresses in modelling this type of energy exchange are slow and limited. The Fleet Numerical Oceanographic Center in Monterey, California, has tested several models and it is quite difficult even to evaluate the results.

3. The energy exchange between the ocean and its bottom and margin is required to be known: The energy included here is the thermal energy and the kinetic energy associated with volcanic actions, and the coastal runoff. Because of the small amount of energy involved, this particular item is usually neglected.

4. The net gain and loss of mass at the air-sea interface, the margin and the bottom of the ocean is required to be known: The net gain and loss

of mass included are the coastal runoff, sinks and sources of water at the bottom of the ocean and the evaporation and the rainfall at the air-sea interface. This type of quantity is usually represented by a term at the right hand side of Equation (2.3b), the equation of continuity. The positive and the negative values for this term represents net gain and net loss of mass, respectively. Unless the area of ocean under investigation is very close to a river the term is usually set to be zero. In other words, Equation (2.3b) is an approximation.

5. The depth of the ocean is required to be known: The ocean circulation expressed by the physical parameter $\vec{q}$ is usually the sum of two major types of currents which are the wind-driven current and the geostrophic current. The other minor types of currents such as thermohaline current and tidal current are quite small in magnitude in the deep ocean. Therefore, the primary concern for acquiring the information on the depth of the ocean is for the calculations of geostrophic and wind-driven currents. The wind-driven current, like the Ekman current [Neumann and Pierson, 1966] which is significant only to a depth not more than 100 meters, decays quite rapidly with increasing depth. Based upon the physical argument by using the scale approximation the wind-driven current can hardly exist beyond the thermocline. Morever, the horizontal pressure gradient which is responsible for the geostrophic current is reduced to zero at some depth beneath the thermocline. The depth can be of the order of 1000 to 1500 meters. Practically speaking the ocean bottom for current calculations can be set at 1000 to 1500 meters in depth. For the portion of ocean whose depth is less than 1500 meters the actual depth of ocean bottom should be provided.

6. The current and the density at the surface of the ocean is required to be provided: By using the satellite-borne radiometer observations in the infrared range with 1°C resolution, Richardson, et al., [1973], Scully-Power, et al., [1975], Voorhis, et al., [1976], Wyrtki [1977], and Bruce [1979] have successfully demonstrated the correlation between the satellite observed ocean surface temperature and the mesoscale eddies, current fronts, and advection patterns. Resolution of 0.5°C

over 10 km area will improve the capability for mapping out the finer structures within the mesoscale features at the ocean surface. As to the information on the ocean surface current, Huang, et al., [1978], and Leitao, et al., [1978a, 1978b, and 1979] are successful, also, in inferring the Gulf Stream, the eddies and their boundaries. The satellite-borne altimeter can infer the geostrophic current at the ocean surface. In the following section, examples will be presented to further illustrate this particular space-borne technique.

However, using undersea acoustics alone, the condition described by Item 2 (which is the energy exchange at the air-sea interface) is not required to be specified. An inverse solution technique proposed by Munk and Wunsch [1979] can be used in areas with large spatial variations in density profiles so that finer spatial resolution can be obtained for these acoustic sensitive areas. In area with small horizontal spatial variations in density profiles, however, this technique tends to be over-determinated.

V. EXAMPLE OF OCEAN SURFACE CURRENT INFERRED BY SPACEBORNE ALTIMETER MEASUREMENTS

From the previous section, Section IV, it is recognized, no matter what numerical approach is taken, that the descriptions on the ocean surface current is one of the required boundary conditions for the determination of the three dimensional density (temperature) field uniquely. The spaceborne altimeter has been suggested, in Section IV, and investigated [Chen, et al., 1980] to be the logical choice for the provision of the required information on the ocean surface current synoptically and globally.

Nevertheless, the basic idea of inferring current by the spaceborne altimeter measurements has three important parts. The first part of idea is the feasibility of observing the mean sea level ζ or the dynamic height $g\zeta$ with the in situ measurements. The second part is the feasibility of observing ζ or $g\zeta$ from the spaceborne platform. The third part, of course, is the feasibility of relating those ζ or $g\zeta$ observed from the spaceborne platform to the ocean surface current. The last

part of the idea has been explained in detail in Sections II and III and, also, by Chen, et al., [1980].

As to the first part, there are many reports and papers, in the open literature, on the evaluations of dynamic heights across currents, and eddies. Vukovich and Crissman [1978] evaluate the two dimensional dynamic topography at the 200 meters depth relative to the 450 meter depth over an eddy. Because there is negligible amount of current motion at the depth of 450 meters level, the 450 meters depth can be considered as the motionless bottom for the geostrophic current calculation. Furthermore, since the current is more or less constant for the first 200 meters beneath the ocean surface at any given horizontal position, the dynamic topography at the ocean surface should be almost identical to that calculated at the 200 meters depth.

Figure 5.1A shows sea lane used by oil tankers en route between Persian Gulf and Atlantic ports along which the expendable bathythermograph (XBT) sections are obtained. Sections of temperature in °C along the tanker sea lane from XBT's for three successive monsoons are shown in Figures 5.1B and 5.1C for 1975, in Figures 5.1D and 5.1E for 1976, and in Figures 5.1F and 5.1G for 1977. The large Somali prime eddy is clearly discernible at 4°N to 12°N, in latitude, with the smaller Socotra eddy to the northeast. The shaded triangular areas off Somali coast are the probable regions of upwelling. Figure 5.2 shows the sea surface dynamic heights for those XBT sections shown in Figure 5.1. The mean salinity is used for the calculations of these dynamic heights. The typical dynamic height shows a change of 5.7 m^2/sec^2 over a distance of 1° in latitude.

Furthermore, over a typical area of ocean, Figure 5.3 shows the two-dimensional sea surface temperature in °C and the two-dimensional surface dynamic height in meters, relative to 1500db, of the MODE area [MODE GROUP, 1978]. The crosshatched area on the maps of dynamic height show all surface water cooler than the mean for the period. The depth of 1500 db is chosen because Schmitz, et al., [1976] determined that 80% of the geostrophic surface current is, on the average, due to density

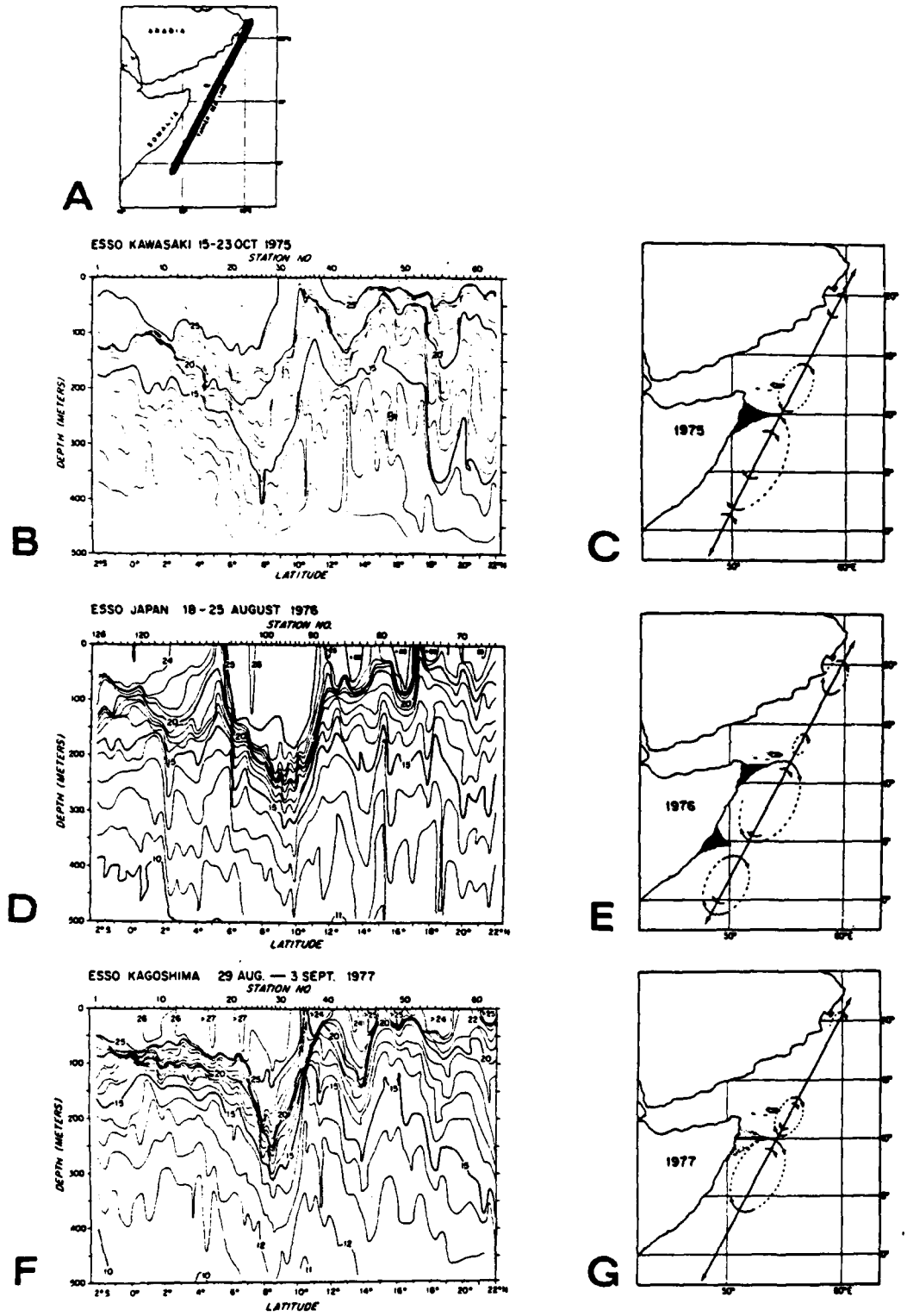

Fig. 5.1 — XBT sections across eddies off the Somali coast [Bruce, 1979].

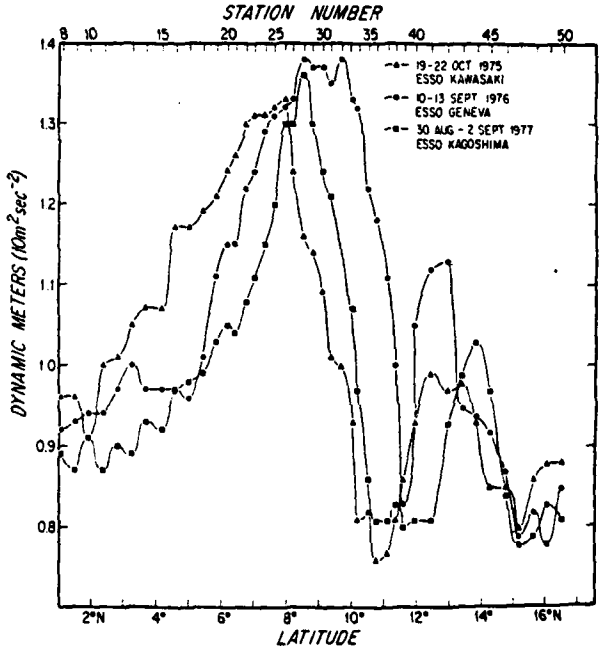

Fig. 5.2 — Sea surface dynamic heights for those XBT sectionsh shown in Figure 5.1 [Bruce, 1979].

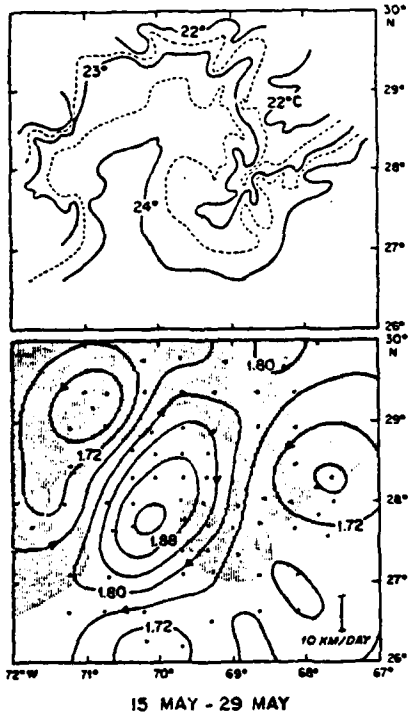

Fig. 5.3 — Sea surface temperature map (upper) in °C and surface dynamic topography (lower) in meters, [Voorhis, et al., 1976].

structure above 1500 m. The direction of geostrophic current is indicated by the arrows and the magnitude can be estimated from the geostrophic speed scale shown in the lower right corner. Therefore, not only the dynamic heights are successfully evaluated one and two dimensionally in the fields, but also these results of dynamic heights are confidently used to calculate the geostrophic current. The first part of the idea is indeed valid and proven.

The second part of idea is related to the spaceborne measurements. Figure 5.4 shows the two dimensional mean sea surface in meters using elevations obtained at each crossing, shown in inset, of the GEOS-3 satellite altimeter, for November 1975. The locations and boundaries of the Gulf Stream are shown in the expected close relationship with those provided by the climatological data. From this type of mean sea surfaces, the geostrophic current speeds can be evaluated for different profiles. Figure 5.5 shows the comparison of dynamic topography and derived velocity component cross track for three repeated altimeter profiles (satellite passes number 1795, 2321, and 2847) acquired over the same ground track during three successive months. The asterisks indicate the western boundaries of the Gulf Stream for these profiles as determined by Experimental Ocean Front Analysis (EOFA) [Leitao, et al., 1978a]. Figure 5.6 shows the Gulf Stream eddy (ring) movement sequence as defined by satellite-borne surface infrared sensor and satellite altimeter from April 1975 to February 1976. Clearly, from Figure 5.6, the satellite altimeter has been shown to be capable in mapping the mesoscale eddies. Therefore, the spaceborne altimeter has the capability to measure the dynamic heights or the mean sea surfaces from which the ocean surface current can be calculated. These figures, from Figure 5.4 to Figure 5.6, have actually confirmed the second part as well as the third part of the idea.

The idea of inferring the ocean surface current from the satellite altimeter measurements is then fully certified for providing the ocean surface current condition for determination of the three dimensional density (temperature) field. With the other conditions satisfied, the

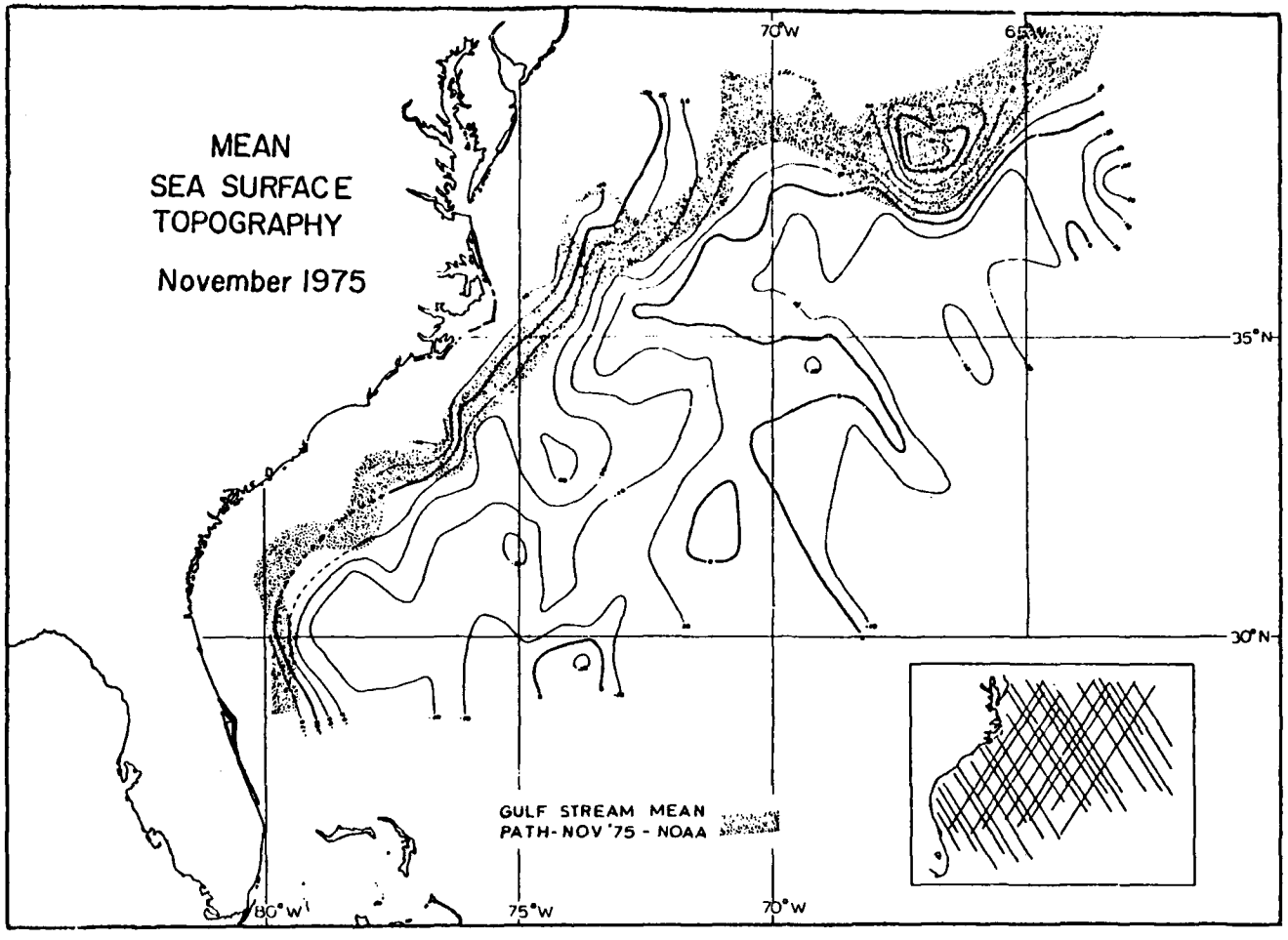

Fig. 5.4 — Mean sea surface topography using elevations obtained at each crossing shown in inset, November 1975 [Huang, et al., 1978].

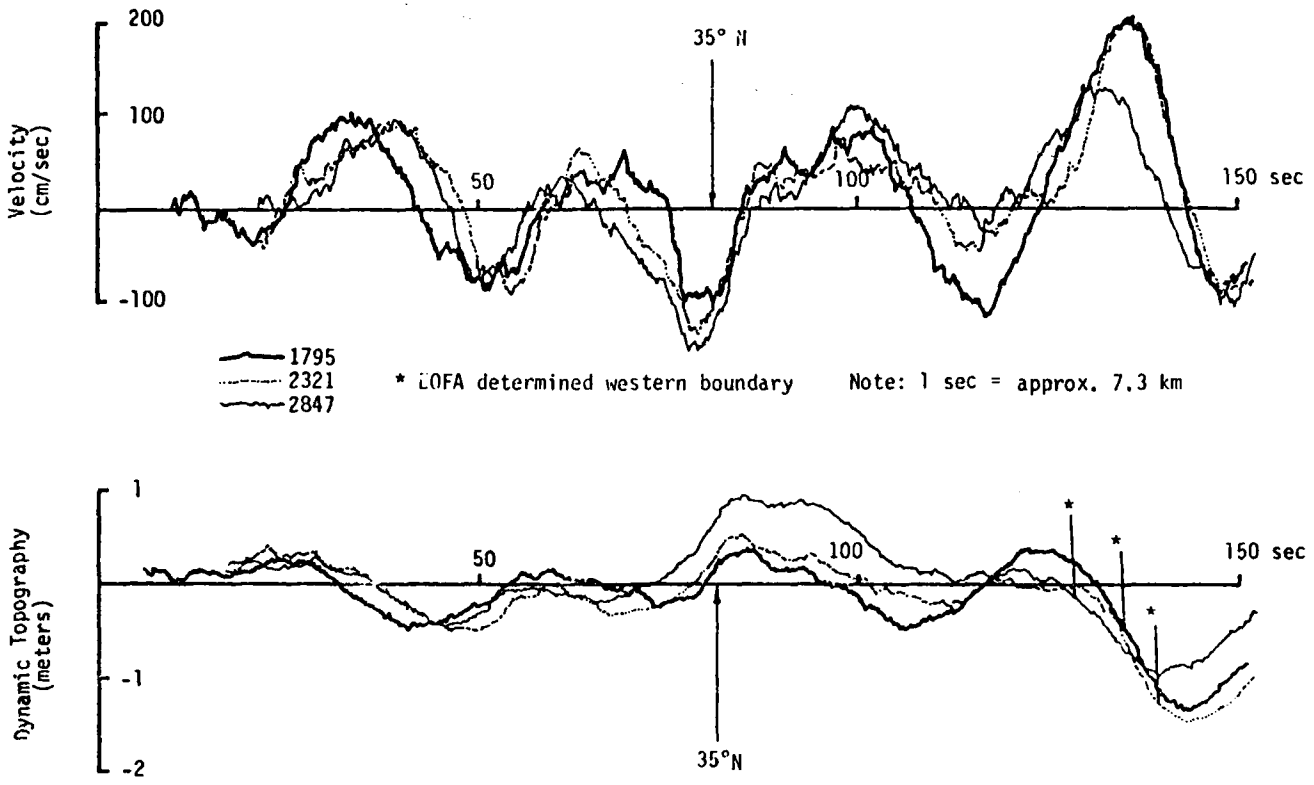

Fig. 5.5 — Comparison of dynamic topography and derived velocity component cross track for three repeated altimeter profiles acquired over the same ground track during three successive months [Leitao, et al., 1978a].

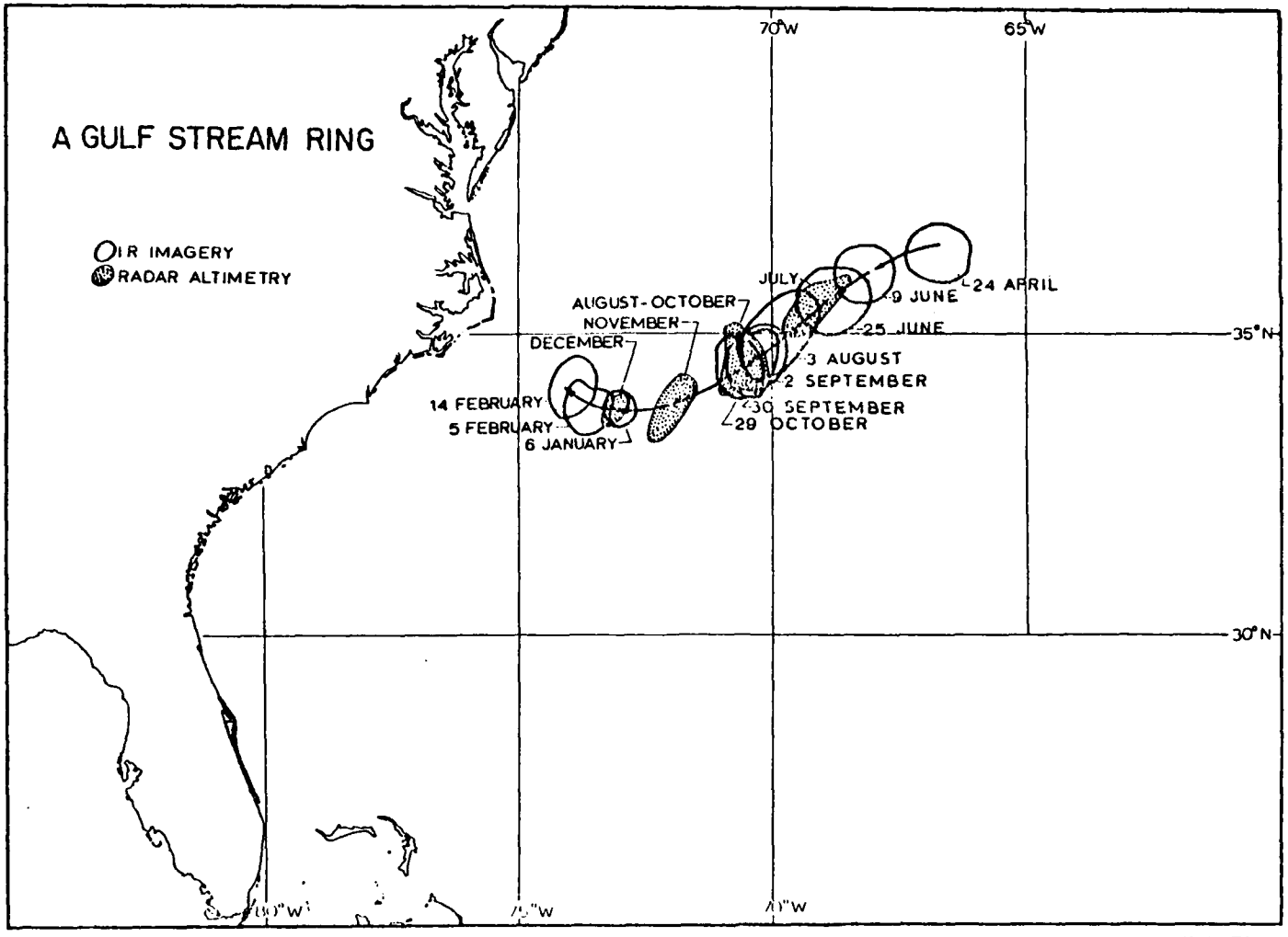

Fig. 5.6 — Gulf Stream ring movement sequence as defined by satellite surface infrare sensor and altimeter, April 1975 to February 1976 [Huang, et al., 1978].

three dimensional (temperature) field determined is unique.

VI. CONCLUSION

In this report the dynamic method used in the field of Physical Oceanography in inferring the geostrophic current and eddy systems has been laboriously developed from its physical theoretical background and its mathematical governing equations for the using of the spaceborne altimeter-sensed dynamic heights or slopes. This method's absolute and relative errors are also discussed briefly.

And, also, the conditions for the determination of the three dimensional density (temperature) field uniquely are mentioned and explained. The spaceborne altimeter is shown to be the instrument for the provision of one condition, i.e., the ocean surface current condition. The three-dimensional density (temperature) field and its boundary conditions at the air-sea interface play dominant roles in the weather prediction and the undersea technology. The interchangeable use of the terms of density and temperature fields is valid only when the salinity can be assumed as constant.

This report should be viewed as complementary to that by Chen, et al., [1980] in which the requirements on the measurement error of the dynamic heights or slopes by the spaceborne altimeter are defined. It is hoped that this report, together with that by Chen, et al., [1980], will help to clearly establish the mission priorities and requirements for future satellite system such as NOSS-2 whose prime missions may include the measurements of current and eddy systems by a spaceborne microwave altimeter.

REFERENCES

Bruce, J.G., Eddies off the Somali Coast During the Southwest Monsoon, Journal of Geophysical Research, Vol. 84, No. C12, 7742-7748, 1979.

Chen, D.T., Smith, S.L., III, and Noble, V.E., On the Measurement of Geostrophic Ocean Current by (Nadir) Satellite Altimeter, In Print, Naval Research Laboratory Memorandum Report, 1980.

Clancy, R.M., and Martin, P.J., The NORDA/SLENUMOCEANCEN Thermodynamical Ocean Prediction System (TOPS): A technical Description, NORDA Technical Note 54, Nov., 1979.

Colquitt, E.S., Malyevac, C.A., and Smith, S.L., III, SEASAT-A Ephemeris Computations, EOS Transections, American Geophysical Union, Vol. 60, No. 18, p. 231, 1979.

Cutting, E., Born, G., Frantrick, J., McLaughlin, W., Neilson, R., and Thielen, J., Mission for SEASAT-A and Oceanographic Satellite, Jet Propulsion Laboratory Document 622-22, 1977.

Emery, W.J., Reid, T.J., DeSanto, J.A., Baer, R.N., and Dugan, J.P., Mesoscale Variations in the Deep Sound Channel and Effects on Low-Frequency and Propagation, Journal of Acoustical Society of America, Volume 66, No. 3, 831-841, 1979

Fomin, L.M., The Dynamic Method in Oceanography, Elsevier Oceanography Series, New York, 1964.

Haiami, S., Kawai, H., and Ouchi, M., On the Theorem of Helland-Hansen And Ekman and some of its applications, Record of Oceanographic Works in Japan, Vol. 2, No. 2, 1955.

Halliwell, G.R., Jr., and Mooers, C.N.K., The Space-Time Structure and Variability of the Shelf Water-Slope Water and Gulf Stream Surface Temperature Fronts and Associated Warm-Core Eddies, Journal of Geophysical Research, Vol. 84, No. C12, 7707-7725, 1979.

Hill, M.N., Editor, The Sea, Volume 1, Physical Oceanography, Interscience Publishers, New York, 1962.

Huang, N.E., Leitao, C.D., and Parra, C.G., Large-Scale Gulf Stream Frontal Study Using GEOS-3 Radar Altimeter Data, Journal of Geophysical Research, Vol. 83, No. C9, 4673-4682, 1978.

Jacobs, W.C., The Energy Exchange between the Sea and the Atmosphere and Some of its Consequences, Bulletin of the Scripps Institute of Oceanography, Vol. 6, 27-122, 1951.

James, R.W., Criticality of Ocean Fronts to ASW Operations, NAVOCEANO Technical Note 7700-3-72, 1972.

Leitao, C.D., Huang, N.E., and Parra, C.G., Remote Sensing of Gulf Stream Using GEOS-3 Radar Altimeter, NASA Technical Paper 1209, 1978a.

Leitao, C.D., Huang, N.E., and Parra, C.G., Final Report of GEOS-3 Ocean Current Investigation Using Radar Altimeter Profiling, NASA Technical Memorandum 73280, 1978b.

Leitao, C.D., Huang, N.E., and Parra, C.G., A Note on the Comparison of Radar Altimetry with IR and In Situ Data for the Detection of the Gulf Stream Surface Boundaries, Journal of Geophysical Research, Vol. 84, No. B8, 3969-3973, 1979.

Levenson, C., and Doblar, R.A., Long-Range Propagation Through the Gulf Stream, Journal of Acoustic Society of America, Vol. 59, 1134-1141, 1976.

McGoogan, J.T., Satellite Altimetry Applications, IEEE Transections, Microwave Theory Technology, Vol. 23, No. 12, 970-978, 1975.

MODE GROUP, Mid-Ocean Dynamics Experiment, Deep Sea Research, Vol. 25, 859-910, 1978.

Munk, W., and Wunsch, C., Ocean Acoustic Tomography: A Scheme For Large Scale Monitoring, Deep Sea Research, Vol. 26A, 123-161, 1979.

Neumann, G., and Pierson, W.J., Jr, Principles of Physical Oceanography, Prentice-Hall, Inc., Englewood Cliffs, N.J., 1966.

Richardson, P.L., Strong, A.E., and Knauss, J.A., Gulf Stream Eddies: Recent Observations in the Western Sargasso Sea, Journal of Physical Oceanography, Vol. 3, 297-301, 1973.

Richardson, P.L., Maillard, C., and Stanford, T.B., The Physical Structure and Life History of Cyclonic Gulf Stream Ring Allen, Journal of Geophysical Research, Vol. 84, No. C12, 7727-7741, 1979.

Schmitz, W.J., Luyten, J.R., Payne, R.E., Heinmiller, R.H., Volkmann, G.H., Tupper, G.H., Dean, J.P., and Walden, R.G., A Description of Recent Exploration of the Eddy Field in the Western North Atlantic with a Discussion of Knorr Cruise 49, Woods Hole Oceanography Institute Technical Paper, 1976.

Scully-Power, P.D., Nysen, P.A., Nilsson, C.S., Twitchell, P.F., Browning, D.G., Swenson, R.C., Andrews, J.C., and Bannister, R.W., A Multisystem Technique for the Detection and Measurement of Warm Core Ocean Eddies, IEEE Ocean '75, 761-768, 1975.

Shear, H.E., Oceanography - Its Implication on ASW, Undersea Technology, 16-19, 1971.

Stommel, H., The Gulf Stream, University of California Press, Berkeley, California, 1966.

Stommel, H., and Yoshida, K., Editors, Kuroshio: Physical Aspects of the Japanese Current, University of Washington Press, Seattle, Washington, 1972.

Tapley, B.D., Schutz, B.E., Marsh, J.G., Townsend, W.F., and Born, G.H., Accuracy Assessment of the SEASAT Orbit and Height Measurement, Report IASOM TR79-5, Institute for Advanced Study in Orbital Mechanics, University of Texas, Austin, Texas, 1979.

Vastano, A.C., and Owens, G.E., On the Acoustic Characteristics of a Gulf Stream Cyclonic Ring, Journal of Physical Oceanography, Vol. 3, 470-478, 1973.

Voorhis, A., Shroeder, E.H., and Leetmaa, A., The Influence of the Deep Mesoscale Eddies on Sea Surface Temperature in the North Atlantic Subtropical Convergence, Journal of Physical Oceanography, Vol. 6, 953-961, 1976.

Vukovich, F.M., and Crissman, B.W., Further Studies of a Cold Eddy on the Eastern Side of the Gulf Stream Using Satellite Data and Ship Data, Journal of Physical Oceanography, Vol. 8, No. 5, 838-845, 1978.

Wyrtki, K., Advection in the Peru Current as Observed by Satellite, Journal of Geophysical Research, Vol. 82, No. 27, 3939-3943, 1977.

ACKNOWLEDGEMENT

The authors would like to thank Dr. J.P. Dugan, a colleague, for his valuable suggestions and also Mrs. Millicent Thompson for the typing of this report. The report is supported by AIRTASK A370-370G/058C/0W05270S00 Program Element 63207N.